An Integrated Likelihood Formulation for Characterizing the Proximity of Position Measurements to Road Segments

Ali Oran, *Member, IEEE,* Patrick Jaillet

***Abstract*—The analysis of spatial proximity between objects can yield useful insights for a variety of problems. A common application is found in map matching problems, where noisy position measurements collected from a receiver on a network-bound mobile object is analyzed for estimating the original road segments traversed by the object. Motivated by this problem, we take a detailed look at proximity measures that quantify the spatial closeness between points and curves in non-deterministic problems, where the given points are noisy observations of a stochastic process defined on a given set of curves. Starting with a critical review of traditional pointwise approaches, we introduce the integral proximity measure for quantifying proximity so as to better represent the statistical likelihoods of a process' states. Assuming a generic stochastic model with additive noise, we discuss the correct proximity function for the proximity measures, and the relationship between a posteriori probabilities of the process and the proximity measures for a comparison of both measures. Later, we prove that the proposed measure can provide better inferences about the process' states, when the process is under the influence of uncorrelated bivariate Gaussian noise. Finally, we conduct an extensive Monte Carlo analysis, which shows significant inference improvements over traditional proximity measures, particularly under high noise levels and dense road settings.**

***Index Terms*—Vehicle Localization, Map Matching, GPS, Integrated Likelihood**

I. Introduction

A. Motivation

Since the beginning of 2000s, with the increasing use of personal navigation assistants (PNAs), and GPS-equipped smart phones, the problem of localizing vehicles/pedestrians on urban road networks has been a major research interest under the generic name of Map Matching (MM). It is of importance to intelligent transportation systems for understanding the travel patterns in a city, or in surveillance systems for tracking mobile objects on a network. It can be considered as a discrete time state estimation problem, and, given that objects are constrained to move along a network, rather than on open space, it may seem at first to be a trivial exercise. However, MM easily becomes challenging, when urban canyons deteriorate position measurements, and when a large number of roads makes it difficult to estimate the original location of the object. Consequently, a good amount of research has been dedicated to it; and various approaches, from simple proximity methods to complex tracking filters, have been proposed (see surveys [1], [2]). In practice, the chosen MM method depends on the application and the available data [3]. Most of the studies have addressed the MM of vehicles equipped with PNAs or similar devices with GPS receivers [4]–[12], which, by using a reliable car battery, can provide frequent and relatively accurate GPS traces. Under such data, the aforementioned studies have been able to deliver good estimations. Another group of studies have considered harnessing additional data sources (e.g. accelerometer, gyroscope) to propose good methods as well [13]–[15]. However, there is still a need for new approaches that can improve the matching accuracy of general MM problems, dealing with estimation of the location of any mobile objects, in the absence of frequently sampled GPS or multiple-sensor data. One of the driving forces for this need is the recent emergence of smart phones as the data sources for understanding urban mobility patterns [16]–[18]. The accuracy limitations of smart phone sensors, and these sensors' reliance on the phone battery, require the next generation MM algorithms to be able to harness low-frequent, and highly-noisy position data [19]–[21]. Motivated by this type of problems, in this paper we introduce more accurate statistical measures to distinguish the possible locations of a road-bound mobile object, through a proximity analysis of its position data with respect to the road network.

B. Problem Statement

In general, when the frequency of the position measurements of a mobile object decreases, the uncertainty about its true locations increases considerably [22], [23]. This situation is more pronounced when the position data is also highly noisy. If additional information is available about the object (e.g speed, acceleration, heading direction) or about the traversed network (e.g traffic speed data on roads), then using data fusion methods or other means, uncertainties could be reduced, and object's original location can be estimated with high accuracy. This type of analysis has been well-studied in the literature, such as the ones incorporating Kalman and Particle Filters [5], [7], [14], [15], [24], or other methods [25]. Meanwhile, the reliance on extra data limits this type of approaches' usage.

A. Oran was with the Future Urban Mobility IRG at Singapore MIT Alliance for Research and Technology Center, 138602, Singapore. He is now with University of Colorado, Boulder, 80303 USA, e-mail: ali.oran@colorado.edu.

P. Jaillet is with Department of Electrical Eng. & Comp. Science (EECS) at MIT, Cambridge, MA 02139 USA, email: jaillet@mit.edu.

This research was supported by the National Research Foundation Singapore through the Singapore MIT Alliance for Research and Technology's FM IRG research program.

In the absence of extra data, localization algorithms need to rely on position data and the road network. Through the analysis of these two data sets, a variety of heuristic weights, probabilities, and criteria have been incorporated, such as the proximity weight, the emission probability, the travel distance criteria, the travel orientation criteria [3], [11], [22], [26]. While such heuristics have contributed to better results in particular studies, their contributions in a generic problem would depend on the validity of the assumptions made for them. For instance, when a position data is observed at similar proximity to some roads, this brings a significant uncertainty for determining the original location of the vehicle. If the position data were sampled frequently, by comparing the possible distances the vehicle could have traversed in that short period, one could estimate the location of the vehicle with fair accuracy. Yet, heuristics of the sampling period can only remain reliable when those periods are low [27]. Under long sampling periods, in order to decide among the numerous possible paths, one has to make strong assumptions about the mobile objects' travel (e.g. traveling only through shortest paths, not making u-turns, or specific route choices such as highways), which may not be generalized. Consequently, the important question is, how to define a quantitative measure for distinguishing the *possibility* among different segments, in the availability of only sparse and noisy position data, and without making a priori assumptions about the object's movement.

In this regard, when analyzing the road segments with respect to given position measurements, one fact is widely accepted: a segment closer to a measurement is more likely to be the true segment for the measurement compared to another segment further away [28]. This simple, yet reliable fact about the spatial closeness between position measurements and the road segments can be referred to as the proximity relation. Analyses based on the proximity relation have been considered in almost every MM method, following the common availability of position measurements, the relation's sampling frequency invariant nature, and particularly its independence from any motion model assumed for the mobile object. Considering these 3 properties, it can be used to define the measure sought in the previous paragraph. Therefore, the critical problem is how to define a measure for the proximity of a segment to a position measurement, so that the likelihood of segments will be well reflected in the measure, and be consistent.

C. Related Work

Several studies have addressed measures of proximity in other problems, where closeness between objects have also been an important consideration, such as clustering, classification, and information retrieval. In contrast, proximity measures haven't got much attention in MM literature, in both probabilistic and deterministic studies. In both groups, various measures that are based on the analysis of a position measurement with respect to road segments' coordinates can be considered as belonging to the class of proximity measures. In this regard, in deterministic MM methods, measures defined by monotonically decreasing functions of the Euclidean distance [12], [22], [26], commonly named as proximity-weight or criteria, are proximity measures. In probabilistic methods, observation (emission) probabilities defined only through the coordinates of the observation and the road segments [29]–[33] are proximity measures as well. While these methods are conceptually different, the proximity formulations have been considerably similar, and simple in most studies in both groups. A proximity function, chosen according to the characteristics of the problem, is used to define the proximity measure of a segment, with some studies also imposing bounds. While a variety of proximity functions have been proposed, almost all are defined by having the (shortest) distance from the observed position to the segment as its argument [6], [10], [12], [20], [22], [26], [29]–[40]. The table of MM methods in [41] shows some of this common pattern. They are easy to compute, as they only require finding the closest point of the segment to the position measurement, and then the corresponding distance. Since shortest distance becomes the sole argument for the proximity measure, we will refer to measures of this kind as "shortest distance based proximity measures".

For a problem like MM that deals with noisy position measurements the sole reliance on the shortest distance can yield inaccurate inferences. A group of segments with very different geometric characteristics would not necessarily be differentiated under such measures. Alternatively, more complex proximity functions, such as the Mahalonobis distance commonly used in nearest neighbor algorithms but rarely used in MM, have also been proposed [42]. Under this approach, a maxima (or minima) of the chosen proximity function along the segment is considered as the proximity measure of the segment. Since the measure is defined as the pointwise extremum of the proximity function, we will refer to this type of measures as "pointwise proximity measures"[1]. While the use of complex proximity functions could be an improvement to the shortest distance based functions, segments of different geometry can again easily be associated with similar proximity values, if their extrema points are similar. Generally speaking, the reliance on a single point of a segment could make any pointwise proximity measure insufficient for reflecting the likelihood of the overall segment.

The very common use of pointwise measures could be attributed to a few factors, most importantly their relatively simple and compact formulations, then, the historic development of MM literature from pure geometric methods, which was based on finding the closest segment to a given point, and, finally, the reliance on other aspects of the input. When data is frequently sampled, or additional data is available, various additional techniques can be quite accurate, and, one can have the luxury to use simple proximity measures, without a significant drop in the accuracy of the overall method. Hence, for the most generic MM algorithms, the only positive aspect of using pointwise measures is their compact formulations.

Consequently, alternative proximity measures have been proposed in [19], [22], [41], [43], [44]. The drawback of these measures are that they have been either brief proposals with

[1]Note that, since the shortest distance is associated with the closest point of a segment to a given point, shortest distance based proximity measures are in fact special cases of the broader group of pointwise measures.

limited scope, or are bound to particular MM algorithms that can not be implemented as stand alone proximity measures in other studies. For instance, a short discussion about the possible drawbacks of the shortest distance based proximity measures was presented by the authors in [43]. An alternative formulation was proposed by cumulating the pointwise Euclidean distance based measures on a segment through a line integral; and a closed form was also developed with a 1-D Gaussian proximity function, and by considering road links' polyline nature. Later, in [45], the proposed formulation was used under a Hidden Markov Model (HMM) based MM algorithm, that had combined the proximity weights with topological transition weights of segments. For the GPS set of [29], the HMM method with the cumulative weights was shown to yield better estimations, particularly in noisy and sparse data sets, compared to the same HMM method with the shortest distance based proximity weights. Yet, these studies have limited scope in formulations and results. In [19], an exponential function of distance between the observation and the segment was used as an observation model. The line integral of the observation probability on possible paths was later used in their recursive MM formulations along with their traffic model. The formulation's solution was dependent on their Domain of Data Relevance (DDR) concept that was proposed in their earlier work [46], and overall lacked a closed form. Frechet distance was also shown to be a reliable proximity measure in [22] and [41]; but being a distance measure between two curves, it can not be used to define a standalone proximity measure for a road segment given a single position measurement. This limits the type of MM methods it can be part of. In [44], the tangent distance of [47] was introduced to MM; but the need to solve a least square problem might become computationally demanding.

Considering the notion of proximity measures in MM, and the drawbacks of the current measures, an alternative framework defining the proximity between position measurements and road segments is proposed in this study. Our development and later comparisons will be as generic as possible so that a large group of MM and other localization methods can use the proposed framework. We will start our discussion, in Section II, by formulating proximity measures. For doing this, we will first formulate the traditional pointwise approaches and discuss their drawbacks in detail. We will then propose a new alternative approach that will better suit non-deterministic problems with a formulation similar to [43], yet without the reliance on Euclidean distance. In Section III, we will discuss the choice of the proximity function for the proposed approach. Considering the 2-dimensional aspect of the problem, in Section IV, we will develop closed formulations for the proposed measure when position measurements are assumed to be observed under the uncorrelated bivariate Gaussian noise process. We will support the proposed measure by proving that it can yield better estimates compared to pointwise measures. To understand the significance of the new measure, we will compare location estimation performances of the proposed formulations against the pointwise formulations, both considering the bivariate Gaussian noise, via extensive Monte Carlo simulations.

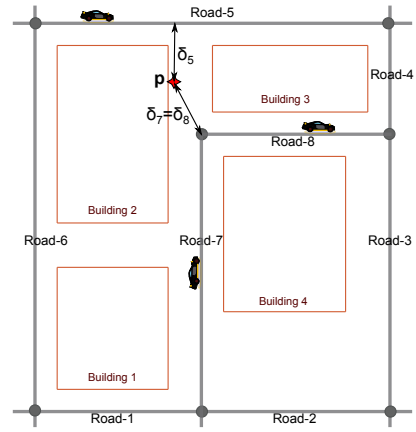

Fig. 1. A typical MM problem on a vector map-like setting. GPS data, p, is almost the same shortest distance ($\delta_5 \approx \delta_7 = \delta_8$) away from a few roads. Shortest distance based proximity measures only considers these distances.

II. Quantification of Proximity

We start our discussion by taking a general look at formulations that define proximity measures between a point and a curve. Remember that our interest is on non-deterministic problems, where the given point is a noisy observation of a stochastic process defined on a set of curves, e.g. position measurements of a road-bound object. We use the terms 'observation' and 'position measurement' as generic terms that encompass coordinate pairs defined on a two dimensional reference frame (e.g. (latitude, longitude) or (north, east) pairs)[2]. We refer to the collection of these position measurements "the spatio-temporal data" of the moving object, and will abstract them under Cartesian coordinates.

We assume that the state space of the stochastic process, the curves in $\mathbb{R}^2$, are well defined and piecewise smooth. A simple piecewise smooth curve can be defined by the parametrized equation, $S \doteq \{s(t) = [x(t), y(t)], t \in [0,1]\}$, where $x(t)$ and $y(t)$ are continuous real valued functions such that $t_1 \neq t_2$ implies, $s(t_1) \neq s(t_2)$, and have piecewise continuous derivatives $\dot{x}$ and $\dot{y}$, where $\dot{x}^2 + \dot{y}^2 \neq 0$ [48]. For brevity, we will refer to simple piecewise smooth curves as curves in the rest of the paper. Also, throughout the paper, we will start our discussion of proximity by first considering curves. We will later consider straight line segments to obtain more tractable results. In MM, this is equivalent to working with vector maps where roads are defined by polylines, which in turn are comprised of straight line segments that are well defined by their end points (shape points) in $\mathbb{R}^2$ (e.g. Fig. 1). In that setting, the set of end points, $\mathcal{V}$, along with the set of line segments, $\mathcal{A}$, form a directed graph, $\mathcal{D} = (\mathcal{V}, \mathcal{A})$. On this graph, it will be possible to define the line segments with their parametrized equations. A segment $S \in \mathcal{A}$, with end points S_A, and S_B in $\mathcal{V}$, can be defined as,

$$S \doteq \{s(t) : s(t) = S_A + t(S_B - S_A), t \in [0,1]\}. \quad (1)$$

[2]Our arguments can be carried to a 3-D MM without loss of generality.

A. Traditional, Point-Wise, Way of Quantifying Proximity

Given a point and a curve in $\mathbb{R}^2$, a measure of proximity between the two can be defined by functions of the Euclidean distance between them. For this discussion, consider points p and s in $\mathbb{R}^2$. Let $d(p,s) : \mathbb{R}^2 \times \mathbb{R}^2 \to \mathbb{R}_{\geq 0}, \mathbb{R}_{\geq 0} \doteq \mathbb{R}^+ \cup \{0\}$, denote the the Euclidean distance between them, i.e., $d(p,s) \doteq ||p-s||$. Accordingly, the (shortest) distance between point p and a curve $S \in \mathbb{R}^2$ can be defined as [49],

$$D(p,S) \doteq \min \{d(p,s) : s \in S)\}. \tag{2}$$

For a general formulation of proximity measures defined by the shortest distance, let $f : \mathbb{R}_{\geq 0} \to \mathbb{R}_{\geq 0}$ be a generic proximity function of distance, assumed to be piecewise continuous, and monotonically decreasing, reflecting the fact that farther away segments to the measurement are less likely to be the true segment. Then, the shortest distance proximity measure of a curve S with respect to a point p can be defined as,

$$f(D(p,S)) = \max_{s \in S} f(d(p,s)). \tag{3}$$

When the curve is a line segment, $D(p,S)$ is the distance from p to its projection on S, if the projection falls on S, or, otherwise it is the distance from p to the closer end point of S [4]. Both cases are shown in Fig. 1, where δ_5, δ_7, and δ_8 are the shortest distances from p_t to roads 5, 7 and 8 respectively. Hence, the proximity measures for roads $5, 7$, and 8 are, $f(\delta_5)$, $f(\delta_7) = f(\delta_8)$, respectively. In practice, a common example of this approach includes the use of the zero-mean one-dimensional Gaussian probability density function (pdf) as the proximity function in probabilistic MM methods. The Euclidean distance becomes the sole argument, yielding,

$$f(D(p,S)) = \frac{1}{\sqrt{2\pi}\,\sigma}\, e^{-\frac{1}{2\,\sigma^2} D^2(p,S)}. \tag{4}$$

Other common formulations include decreasing affine functions of Euclidean distance in deterministic methods.

This type of formulations is easily computable and can provide adequate measures for reflecting the spatial closeness of a curve to a point for some problems. However, in a non-deterministic problem like MM, the use of shortest Euclidean distance as the sole argument as in (3) has drawbacks. First, notice that the Euclidean distance is an isotropic distance measure, i.e., measurements in x and y coordinates are treated equally. Hence, its usage implicitly assumes an isotropic noise distribution, and would yield a subpar proximity analysis if the noise channels are unequal. For instance, in Fig. 1 with shortest distances $\delta_5 \approx \delta_7$, almost the same proximity weights would be assigned to segments $5, 7$ and 8 under piecewise continuous proximity functions, independent of the noise acting on measurements.

Therefore, better measures may be obtained by using proximity functions that can take into account the noise factors inherent in measurements. With this change, rather than finding the shortest Euclidean distance to maximize the distance dependent function f, one would need to find the maximum of a proximity function defined along the curve. To formulate this more general approach, let us introduce $F : \mathbb{R}^2 \times \mathbb{R}^2 \to \mathbb{R}_{\geq 0}$, a generic function that assigns a proximity measure between two points. Then, the pointwise proximity measure of a curve S with respect to a point p can be defined as, [3]

$$W_P(p,S) = \max_{s \in S} F(p,s). \tag{5}$$

In practice, statistical functions, such as Mahalonobis distance or similar forms can be used to define F . For instance, the reciprocal of squared Mahalonobis distance could be used in (5), by considering the covariance of the noise distribution, Σ,

$$F(p,s) = \frac{1}{(p-s)^T\, \Sigma^{-1}\, (p-s)}. \tag{6}$$

However, a significant issue still remains, and that is the complete reliance on particular points of a segment (the extrema points in (5)) for defining the proximity measure of the whole segment. This ignores the variations in proximity function, F, along the segment, which needs to be taken into account if an accurate characterization of the segment's proximity is the goal. Except trivial cases that result in constant F, this reliance would otherwise be equivalent to making an implicit assumption that the extremum point should be the only point of interest in a segment. In MM, this would be equivalent to assuming that the only possible location of the mobile object is on a particular point of the road. Because of the randomness of position measurements, this can not be justified. Hence, the primary drawback of pointwise measures is not about the chosen proximity function, but in fact their reliance on a single point for characterizing a 1-dimensional object. Therefore, in order to define proximity measures that would reflect the likelihoods of segments, this dependency should be addressed first.

B. An Alternative Way for Quantifying Proximity

The dependence on a single point of a curve can be improved by defining measures that take into account the proximities of other points of the curve. For instance, very simply, in addition to considering the maximum as in (5), the minimum of the proximity function can also be considered to define a measure, e.g. the average proximity. Ideally, all points of a curve can be considered to define a complete measure for the curve [4]. In this regard, it would be reasonable to define the proximity measure of a curve as the sum of the measures of points that define the curve. That sum would be defined by a line integral. Hence, the overall proximity measure of a curve S with respect to a point p can be alternatively defined as,

$$W_I(p,S) \doteq \int_S F(p,s)\, dl, \tag{7}$$

with some proximity function $F : \mathbb{R}^2 \times \mathbb{R}^2 \to \mathbb{R}_{\geq 0}$. For the special case of isotropic noise distributions, one can revert to the simpler shortest distance based formulation of [43],

$$\mathcal{W}_I(p,S) \doteq \int_S f(d(p,s))\, dl. \tag{8}$$

[3]Proximity measures are commonly referred as proximity weights in MM literature. Hence we use the notation W for these measures.

[4]In fact, this would be a similar approach to the average linkage approach in clustering algorithms, which considers not only the closest and furthest but all points making up the clusters.

Different than (5), (7) quantifies proximity by considering all points of a curve; and with this consideration, different segments can be distinguished under the proposed measure, e.g. roads $5, 7$ and 8 in Fig. 1 eventually getting different measures. If formulated through the correct proximity function, (7) has the potential to yield measures reflecting the likelihoods of the segments, which will be discussed in III.

At this point, it can be argued that even if the proposed formulation of (7) can yield better measures, the computational effort needed to evaluate the line integral can well offset the possible gains. However, simple smooth curves can be approximated as a union of straight lines. Therefore, it is possible to accurately approximate (7) by a sum of integrals defined on straight segments, e.g. approximating arbitrary shaped roads as a union of straight road segments. In this regard, recall the parameterized form of a line segment $S \in \mathcal{A}$ from (1). Let us introduce vectors, L, R^A, and R^B; the vector defining the segment, and the vectors defining the segment's end points with respect to the measurement point, p,

$$L \doteq S_B - S_A, \quad R^A \doteq S_A - p, \quad R^B \doteq S_B - p. \tag{9}$$

Then, the parametrized equation in (1) can be written as,

$$s(t) = S_A + L\,t, \quad \text{and} \quad \left|\left|\frac{d\,s(t)}{dt}\right|\right| = ||L||. \tag{10}$$

Hence, (7) becomes,

$$W_I(p, S) \doteq ||L|| \int_0^1 F(p, s(t))\,dt, \tag{11}$$

for a straight segment S. Consequently, the proximity weight of a polyline road segment, $\mathcal{P}$, can be found by the sum of the weights of straight line segments constituting it,

$$W_I(p, \mathcal{P}) \doteq \sum_{S_i \in \mathcal{P}} ||L^{S_i}|| \int_0^1 F(p, s(t))\,dt. \tag{12}$$

Equation (11) can be computed easily by numerical integration methods, particularly when working with piecewise continuous proximity functions. Therefore, the needed computational effort for the proposed measure can be kept minor in most problems. In fact, it is possible to develop closed form solutions to (11) for certain proximity functions, as will be discussed in IV.

III. The Choice of Weight Function

Now that the underlying formulations of our approach have been defined, with (7) for any curve, and (11) for straight segments, we proceed to discussing the choice of the proximity function, F. Since the proximity measures are expected to reflect the likelihoods of segments, considering functions that can take into account the noise characteristics in position measurements would be necessary. In that respect, we now argue that choosing the pdf of the noise as the proximity function, as in (4), would be needed.

For this discussion, let us develop an observation model for the mobile object. Consider $\mathcal{S} \doteq \{S_i\}$, a finite set of curves in $\mathbb{R}^2$ with at most a finite number of intersection points between each other. We will consider the object's motion as a discrete time stochastic process $\{\xi_k,\, k \in K\}$, taking values on the union set of points that define each segment, and with some index set K. When the noise process, $\{\zeta_k\}$ is additive, the observation at k can be formulated as, $z_k = \xi_k + \zeta_k$.

Consequently, the likelihood of process ξ_k with state $s \in S$, $S \in \mathcal{S}$, generating the observation $z_k = p$ would be, $g_\zeta(p-s)$, where g_ζ is the pdf of the noise. Hence, by choosing the proximity function, F, as g_ζ, a proximity measure can reflect the likelihoods of stochastic processes' states. In our problem, considering the statistical likelihoods of all points of a segment through the line integral, (7), a whole segment's likelihood could be represented in the resulting measure. This can be interpreted as an integrated likelihood formulation for proximity. Hence,

$$W_I(p, S) \doteq \int_S g_\zeta(p - s)\,dl, \tag{13}$$

for any curve S, and

$$W_I(p, S) \doteq ||L|| \int_0^1 g_\zeta(p - s(t))\,dt, \tag{14}$$

for a line segment are the proposed integral proximity measures of a segment with respect to a point. In comparison, the pointwise formulation of (5) becomes,

$$W_P(p, S) = \max_{s \in S} g_\zeta(p - s). \tag{15}$$

In order to get more insight about these measures, let us take a look at the a posterior probability of the mobile object being on a particular curve S given an observation p at some time k, $Pr(\xi_k \in S \,|\, z_k = p)$. Remember that the curves can only have a finite number of intersection points. So, the probability of ξ_k being on these points is zero. Hence, we can omit them without loss of generality, and consider $\mathcal{S}$ as a union of disjoint segments. Using Bayes rule,

$$\begin{aligned} Pr(\xi_k \in S \,|z_k = p) &= \frac{Pr(\xi_k \in S, z_k = p)}{Pr(z_k = p)} \\ &= \frac{Pr(z_k = p \,|\, \xi_k \in S)\, Pr(\xi_k \in S)}{\sum_{S_i} Pr(z_k = p \,|\, \xi_k \in S_i)\, Pr(\xi_k \in S_i)}. \end{aligned} \tag{16}$$

In (16), the denominator is a constant independent of the particular segment, and can be omitted .

$Pr(z_k = p \,|\, \xi_k \in S)$ is the observation probability of p given the process being on curve S. Remember that, we have defined a curve S as a set of points. Therefore,

$$\begin{aligned} Pr(z_k = p \,|\, \xi_k \in S) &= \frac{Pr(z_k = p, \xi_k \in S)}{Pr(\xi_k \in S)} \\ &= \frac{1}{Pr(\xi_k \in S)} \int_S g_{z,\xi}(z_k = p, \xi_k = s)\,dl \\ &= \int_S g_{z|\xi}(z_k = p \,|\xi_k = s)\, g_\xi(\xi_k = s \,|\xi_k \in S)\,dl. \end{aligned} \tag{17}$$

In (17), $g_{z|\xi}(z_k = p \,|\xi_k = s) = g_\zeta(p - s)$, and like mentioned above is the likelihood of state being a particular point s while generating data p. The second term, $g_\xi(\xi_k = s \,|\xi_k \in S)$, is the conditional prior density of state being s, given that state is in S. Regarding this term, note the probabilistic MM methods' definition of observation probability, $Pr(z_k = p \,|\, \xi_k \in S)$,

as the likelihood for a particular point of state space, that is, $g_{z|\xi}(z_k = p \,|\, \xi_k = s^*)$ for some $s^* \in S$. This is an implicit assumption that the moving object was almost certainly on s^*, i.e. in (17) the conditional a priori would be implicitly assumed as,

$$g_\xi(\xi_k = s \,|\, \xi_k \in S) = \begin{cases} 1 & \text{for } s = s^*, \\ 0 & \text{else.} \end{cases} \tag{18}$$

As mentioned earlier, this strong assumption rules out the possibility of the object being on another point of the segment. When observation probability is defined without incorporating the dynamics of the object, or without the availability of a priori information about its position, a better approach would be to assume a uniform probability among the points that make up the segments. Hence, rather than (18), the conditional a priori can be defined as the inverse of the segment's length,

$$g_\xi(\xi_k = s \,|\xi_k \in S) = \frac{1}{||L||}, \quad \forall\, s \in S, \forall S \in \mathcal{S}. \tag{19}$$

In (16), $Pr(\xi_k \in S)$ is the a priori probability of the whole segment, and can be formulated in a number of ways, the most common by conditioning on the previous possible states [50],

$$Pr(\xi_k \in S) = \sum_i Pr(\xi_k \in S \,|\, \xi_{k-1} \in S_i) Pr(\xi_{k-1} \in S_i),$$

or, if available, conditioning on the set of previous observations up to time $k-1$, that is $\{Z\}^{k-1}$,

$$Pr(\xi_k \in S \,|\{Z\}^{k-1}) = \sum_i Pr(\xi_k \in S \,|\xi_{k-1} \in S_i, \{Z\}^{k-1}) \\ Pr(\xi_{k-1} \in S_i \,|\, \{Z\}^{k-1})).$$

Notice that both equations are dependent on the assumed dynamic model for the process, $Pr(\xi_k \in S \,|\, \xi_{k-1} \in S_i)$. Yet, since we are looking at a generic stochastic process, we will avoid considering a specific model that can favor some segments. Therefore, we consider $Pr(\xi_k \in S)$ independent of previous states and observations, and define it under uniform probability. Under this approach, there are two possible formulations. The first one accepts a uniform probability distribution among the segments,

$$Pr(\xi_k \in S) = c, \quad c \geq 0, \quad \forall S \in \mathcal{S}, \tag{20}$$

whereas, the other accepts a distribution dependent on the size of the state space at each segment,

$$Pr(\xi_k \in S) = \frac{||L||}{\sum_i ||L^{S_i}||} \propto ||L||, \quad \forall S \in \mathcal{S}. \tag{21}$$

To decide between the two, the modeler needs to assess if a longer segment has a higher probability to be the original location of a mobile object compared to a shorter one, before observing the data. This point is illustrated in Fig. 2. Note that, the consideration of segment length in (21) along with (19) is equivalent to assuming equal probability for all points of the state space, whereas (20) with (19) implies higher probability for the points belonging to shorter segments. In order to avoid such bias, we continue our derivation with (21). [5]

[5]Continuing with (20) wouldn't affect our preceding discussions neither. In that case, only the segment length from (21) would be omitted. Hence, the a posteriori formulations would still be similar to (23) and (24), only the right hand terms would both have a factor of $1/||L||$.

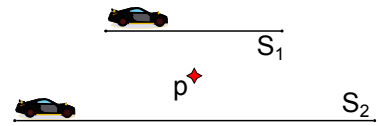

Fig. 2. State space of 2 segments of different lengths. Should a priori probabilities satisfy $Pr(\xi \in S_1) = Pr(\xi \in S_2)$ or $Pr(\xi \in S_2) > Pr(\xi \in S_1)$?

Plugging (17) into (16), the a posteriori equation becomes,

$$Pr(\xi_k \in S \,|\, z_k = p) \propto Pr(\xi_k \in S) \\ \int_S g_{z|\zeta}(z_k = p \,|\xi_k = s)\, g_\xi(\xi_k = s \,|\xi_k \in S)\, dl. \tag{22}$$

Considering the uniform probability of points on a segment in (19), and the a priori formulation of (21),

$$Pr(\xi \in S \,|\, z = p) \propto \int_S g_\zeta(p - s)\, dl. \tag{23}$$

Here, notice the similarity between (23) and (13). The measure proposed in (7) in fact reflects the a posterior probability of a stochastic process, when the proximity function F is chosen as the pdf of noise acting on the process, and when uniform a priori assumptions are made about the process' possible locations. Under the pointwise approach, with the choice of the a priori being (18) rather than (19), we would have got a particular point's likelihood for the posterior probability:

$$Pr(\xi \in S \,|\, z = p) \propto g_\zeta(p - s^*). \tag{24}$$

Hence, the integral proximity measure would benefit the characterization of proximity between curves and points. For certain groups of probability distributions and curves the improvements can be proven to be valid independent of position data, curves' geometry or noise levels.

IV. Comparison of Proximity Measures Under Uncorrelated Bivariate Gaussian Noise

Studies have shown that errors in GPS measurements can be modeled under a Gaussian distribution [28]. Accordingly, it has been very common in MM studies to assume a 1-D zero-mean Gaussian noise distribution. Here, we also assume a Gaussian based noise model, but rather an uncorrelated bivariate Gaussian distribution because of the 2-D nature of MM problem.

A. Theoretical Development

Let us consider an uncorrelated bivariate Gaussian noise process with pdf $g_\zeta \sim N(0, \Sigma)$, where

$$\Sigma \doteq \begin{bmatrix} \sigma_1^2 & 0 \\ 0 & \sigma_2^2 \end{bmatrix}, \text{hence } |\Sigma| = \sigma_1^2\, \sigma_2^2,\ \Sigma^{-1} = \begin{bmatrix} \frac{1}{\sigma_1^2} & 0 \\ 0 & \frac{1}{\sigma_2^2} \end{bmatrix}.$$

In this setting, let us define the normalized forms of vectors R^A, R^B, and L (from (9)),

$$\tilde{R}^A \doteq \begin{bmatrix} [R^A]_1 / \sigma_1 \\ [R^A]_2 / \sigma_2 \end{bmatrix},\ \tilde{R}^B \doteq \begin{bmatrix} [R^B]_1 / \sigma_1 \\ [R^B]_2 / \sigma_2 \end{bmatrix}, \tag{25}$$
$$\tilde{L} \doteq \begin{bmatrix} [L]_1 / \sigma_1 \\ [L]_2 / \sigma_2 \end{bmatrix};$$

and the unit vector along $\tilde{L}$,

$$\tilde{l} \doteq \tilde{L}/||\tilde{L}||. \tag{26}$$

Lemma 1. *Under an uncorrelated zero-mean bivariate Gaussian noise process with pdf $g_\zeta \sim N(0,\Sigma)$, the integral proximity measure for a straight line $S \in \mathbb{R}^2$,* (14)*, can be formulated in the following compact form,*

$$W_I(p,S) = \frac{1}{\sqrt{2\,\pi}\,\sigma_1\sigma_2}\, c(S)\, w^{\perp}(p,S)\, w^{\parallel}(p,S), \tag{27}$$

where,

$$c(S) \doteq ||L||/||\tilde{L}|| \tag{28}$$

is a geometry factor for the segment, independent of observed data p,

$$w^{\perp}(p,S) \doteq e^{-||\tilde{R}^A_{\tilde{L}^\perp}||^2/2}, \tag{29}$$

$$w^{\parallel}(p,S) \doteq \Phi(\tilde{R}^B\cdot\tilde{l}) - \Phi(\tilde{R}^A\cdot\tilde{l}), \tag{30}$$

are functions of perpendicular and parallel projections of data vectors $\tilde{R}^A$ and $\tilde{R}^B$ on vector $\tilde{L}$, that is,

$$\tilde{R}^A_{\tilde{L}^\perp} \doteq \tilde{R}^A - \tilde{R}^A_{\tilde{L}^\parallel}, \quad \tilde{R}^A_{\tilde{L}^\parallel} \doteq (\tilde{R}^A\cdot\tilde{l})\,\tilde{l}, \tag{31}$$

Φ being the Gaussian cumulative distribution function.

Proof. See Appendix A. □

In (27), notice the separate contributions of orthogonal and parallel projections of data vectors, and the shape factor $c(S)$. In comparison, the following lemma presents the compact form of the pointwise proximity measure of (6).

Lemma 2. *Under an uncorrelated zero-mean bivariate Gaussian noise process with pdf $g_\zeta \sim N(0,\Sigma)$, the pointwise proximity measure for a straight line $S \in \mathbb{R}^2$,* (15) *can be formulated in the following compact form,*

$$W_P(p,S) = \frac{1}{2\,\pi\,\sigma_1\sigma_2}\, v(p,S), \tag{32}$$

where,

$$v(p,S) = \begin{cases} e^{-||\tilde{R}^A||^2/2} & \text{if } (\tilde{R}^A\cdot\tilde{l}) \geq 0, \\ e^{-||\tilde{R}^B||^2/2} & \text{if } (\tilde{R}^A\cdot\tilde{l}) \leq -||\tilde{L}||, \\ e^{-||\tilde{R}^A_{\tilde{L}^\perp}||^2/2} & \text{else,} \end{cases} \tag{33}$$

depends on where the data point's projection on $\tilde{L}$ falls onto. The last one corresponds to the case when the projection falls onto $\tilde{L}$, and the first two corresponds to cases when the projections fall outside.

Proof. See Appendix B. □

In both (27) and (32), the first terms are independent of segments. Hence, they can be omitted if the likelihood comparison of some segments is the only goal. For such comparisons, the following theorem shows a better expected accuracy for the integrated likelihood proximity measure. We omit the time indices for the stochastic process, because of the time-invariant nature of proximity measures.

Theorem 1. *Let $\mathcal{S} = \{S_i\}$ be a collection of non-overlapping straight line segments in $\mathbb{R}^2$. Let ξ be a stochastic process taking values on the union of the sets of points that define each segment of $\mathcal{S}$ with uniform probability. Assume that ξ is observed under an additive noise process ζ, yielding observation, $z = \xi + \zeta$.*

To estimate the original segment of some observation $z = p$, consider estimators E^P based on (5)*, and E^I based on* (7)*, with a common proximity function $F : \mathbb{R}^2 \times \mathbb{R}^2 \to \mathbb{R}^+$,*

$$E^P(p,\mathcal{S}) \doteq \underset{S\in\mathcal{S}}{\operatorname{argmax}}\, W_P(p,S) = \underset{S\in\mathcal{S}}{\operatorname{argmax}} \left[\max_{s\in S}\left(F\left(p,s\right)\right)\right], \tag{34}$$

$$E^I(p,\mathcal{S}) \doteq \underset{S\in\mathcal{S}}{\operatorname{argmax}}\, W_I(p,S) = \underset{S\in\mathcal{S}}{\operatorname{argmax}} \left[\int_S F\left(p,s\right)\, dl\right]. \tag{35}$$

If the pdf of ζ, g_ζ, is a zero-mean uncorrelated non-degenerate bivariate Gaussian, then by taking $F(p,s) = g_\zeta(p-s)$, $E^I(p,\mathcal{S})$, and $E^P(p,\mathcal{S})$ would yield unique results almost surely. In addition, the unique results would satisfy,

$$Pr(E^I(p,\mathcal{S}) = S^p) \geq Pr(E^p(p,\mathcal{S}) = S^p), \tag{36}$$

where S^p is the original segment of observation p, i.e., $\xi \in S^p \in \mathcal{S}$.

Proof. See Appendix C. □

The above theorem shows that the proposed integral measure (27) is expected to yield better estimations for the true location of a mobile object compared to the pointwise measure (32) for any position data with any noise level or any road network configuration. The only thing that remains to be seen is whether the proposed measures' improvements could be significant, and if so under what conditions. Yet, depending on the position data, the configuration of road segments, and noise characteristics potential improvements can vary greatly, making it impossible to develop tight analytical bounds on them, while covering all possibilities. Hence, to understand potential gains, performances of both measures needs to be compared numerically under various segments and noise configurations (instances). In the following subsection we will present a detailed analysis of possible gains with a systematic study. Before that, notice the following simplified forms of (27) and (32) under the commonly assumed uniform Gaussian distribution.

Corollary 1. *In the case of uniform noise, $\sigma_1 = \sigma_2 = \sigma_o$,* (27) *simplifies to,*

$$W^o_I(p,S) = \frac{1}{\sqrt{2\,\pi}\,\sigma_o}\, w^{\perp^o}(p,S)\, w^{\parallel^o}(p,S), \tag{37}$$

where,

$$w^{\perp^o}(p,S) \doteq e^{-||R^A_{L^\perp}||^2/(2\,\sigma_o^2)}, \tag{38}$$

$$w^{\parallel^o}(p,S) \doteq \Phi\left(\frac{R^B\cdot l}{\sigma_o}\right) - \Phi\left(\frac{R^A\cdot l}{\sigma_o}\right), \tag{39}$$

are functions of perpendicular and parallel projections of data vectors R^A and R^B on vector L,

$$R^A_{L^\perp} \doteq R^A - R^A_{L^\parallel}, \quad R^A_{L^\parallel} \doteq (R^A\cdot l)\, l, \tag{40}$$

and $l \doteq L/||L||$, being the unit vector along L.

On the other hand, (32) *simplifies to,*

$$W_P^o(p,S) = \frac{1}{2\,\pi\,\sigma_o^2}\, v^o(p,S), \tag{41}$$

where,

$$v^o(p,S) = \begin{cases} e^{-||R^A||^2/(2\sigma_o^2)} & \textit{if } \ (R^A \cdot l) \geq 0, \\ e^{-||R^B||^2/(2\sigma_o^2)} & \textit{if } \ (R^A \cdot l) \leq -||L||, \\ e^{-||R^A_{L^\perp}||^2/(2\sigma_o^2)} & \textit{else,} \end{cases} \tag{42}$$

is a function of the shortest distance between p *and* S*,* $D(p,S)$*.*

Proof. Follows the substitution of σ_o for both σ_1 and σ_2 in equations from (25) through (33). □

B. Estimation Comparison through Monte Carlo Analysis

There are no globally accepted MM data sets for the comparison of different approaches, even though some specific data sets have been made available online. Since the proposed proximity measures are aimed to be a unifying approach for the most general MM problem, we have decided to base our comparisons independent of particular data sets or networks to avoid possible bias. For this purpose, we have worked on randomly generated groups of segments confined to a square test bed of size 200 by 200 units (the length units have been considered analogous to meters). The control parameters for the tests have been chosen to reflect the major factors that can affect proximity measures' accuracy in practice. These are: road networks' sparsity, road segments' length variations, and the severity and anisotropy of the noise. Accordingly, the parameters of interest for the segments are: the number of segments confined to the simulation area, the segments' average length, and the standard deviation of the length of the segments, which is defined through the dimensionless coefficient of variation (CV), the ratio of standard deviation to mean. For the noise: the standard deviation values of the bivariate Gaussian in x and y directions, and their respective ratio (R), are the control parameters of interest. These parameters are summarized in Table I, and Table II.

Each combination of control parameters in Table I defines a particular segment configuration on the test bed. For each configuration, a group of segments were randomly generated; and we call such a group, an instance of segments. On each instance, the performances of both proximity measures have been compared under a Monte Carlo (MC) analysis. In this regard, the stochastic process, ξ, was sampled uniformly on each segment a certain number of times that was proportional to the segment's length (1000 samples per unit length for stable results). This ensured our simulations did not favor a segment or points of the state space. These samples were later corrupted with zero mean uncorrelated bivariate Gaussian noise, with the noise control parameters listed in Table II. (34) and (35) has been used to estimate the original segment of each sample. For comparison, we define the percentage of absolute change in estimation (PACE), and the percentage of relative change in estimation (PRCE), both of which are indicative of the possible gains when integrated proximity is used:

$$\text{PACE} \doteq 100 \times (N_I - N_P)/N, \tag{43}$$

$$\text{PRCE} \doteq 100 \times (N_I - N_P)/N_P, \tag{44}$$

TABLE I
SEGMENT CONTROL PARAMETERS IN SIMULATIONS

	1st Group of Sims.	2nd Group of Sims.
Number of Segs.	$4, 8, 16$	$4, 8, 16$
Av. Length of Segs. (L^μ)	40, 60	20, 40, 60
CV	0.25, 0.5	0, 0.25, 0.5, 1.0

TABLE II
NOISE CONTROL PARAMETERS IN SIMULATIONS

	Uniform Noise Sims.	Non-Uniform Noise Sims.
σ_x	10, 20, 40, 60, 80, $100, 120$	10, 20, 40, 60, 80, 100, 120
$R = \sigma_y/\sigma_x$	1	0.2, 0.5, 0.7

where N is the total number of position samples generated with the MC simulation, N_I is the number of correct position estimates with the integral proximity measure, N_P with the pointwise measure. PRCE has been the primary quantity for observing the trends in gains. But, when N_P becomes low under high noise levels, PRCE becomes quite high. Therefore, we also present PACE to give the reader a better perspective on the gains. In addition, in order to avoid reaching conclusions from a single instance, we have generated 8 random instances for each segment configuration, and present the possible gains (PACE and PRCE) as an average of the gains on 8 instances. For clarity, two instances of randomly generated segments with different segment configurations are shown in Fig. 3.

The first group of simulations have been conducted on groups of segments that belong to transportation-network like graphs, so that these simulations can reflect possible gains on urban road networks. The graphs were generated by a modified version of the 'random geometric graph generator' of NetworkX library [51], which places a number of nodes uniformly at random in the unit cube, and connects any two nodes with an edge if the Euclidean distance between them is lower than a user-defined threshold. We also introduced lower and upper limits on the degrees of nodes, so that the generated graphs would resemble urban road networks rather than abstract graphs. For avoiding a possible bias in segment configurations, a secondary, larger, group of simulations have also been conducted on non-intersecting randomly generated segments. As before, these segments have also been generated by choosing segments' end nodes uniformly at random. Also, only the segments longer than 2 units of length were considered to relate to actual road segments.

While $R \doteq \sigma_y/\sigma_x$ can vary between 0 to infinity, because of the symmetric nature of the covariance matrix and the simulations we have built, analyzing it from 0 to 1 would be sufficient. Still, simulating all the configurations of Table I, for all R values in Table II would be extremely time consuming. Hence, uniform noise simulations were done under all segment configurations, but the non-uniform noise simulations were done only on segment configurations where our proximity measure had resulted in the most gains under the uniform noise. This was done to see if the maximum gains under uniform noise would deteriorate under non-uniform noise.

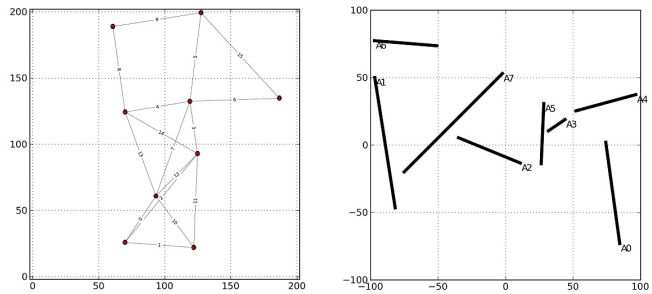

(a) Randomly generated network of 16 segments with mean length of 60, and sample deviation of 15 units.

(b) Randomly generated 8 segments with mean length of 60, and sample deviation of 30 units.

Fig. 3. Two instances of randomly generated segments.

Uniform noise simulations compare measures (37) and (41). The results of our first group of simulations, on road network like segments, are shown in Fig. 4, with 4a showing PRCE, and 4b PACE results. In all subfigures, x-axis shows the uniform standard deviation, $\sigma_x = \sigma_y$, whereas y-axis shows the percent change in estimation. The rows of subfigures corresponds to simulations done on the groups of segments with average lengths, L^μ, of 40, and 60 units; and the columns correspond to simulations with CV values of 0.25 and 0.5. The 3 curves in each subfigure with different colors correspond to the number of segments in the simulation area, blue for 4 segments, red for 8 and green for 16. The results of the second group of simulations on non-intersecting random segments are shown in Fig. 5a and in 5b in a similar fashion with rows corresponding to different average segment lengths, and columns corresponding to different CVs.

From the subfigures in Fig. 4a and Fig. 5a, similar patterns can be observed. The most noticeable pattern is the increase in gains with the increasing CV values, except the case when CV$= 0$, which is the highly unlikely case of all equal length segments. With the increasing variation in segment lengths, a considerable increase in gains can be noticed, with absolute gains up to 18%, and relative gains up to 80% possible. This pattern can be attributed to the relative emphasis of pointwise and integral proximity formulations. Pointwise proximity estimator under uniform noise picks the nearest segment to a measurement as the original segment. The integral proximity estimator, by assuming a uniform probability among all the points of all segments, will consider longer segments more likely compared to shorter ones. Therefore, when the variation between segment lengths increases, the pointwise proximity will never differentiate the likelihood between a short and a long segment, whereas the integral proximity will.

Another pattern is the increase in gains with the increasing noise standard deviation values, again except for the marginal all equal length case. This increase is related to the scattering of position measurements farther away from their original locations on segments with increasing noise levels. When position measurements are not scattered far, both estimators can do well. But, when the measurements are scattered far away, both proximity measures will suffer. However, the pointwise proximity will do worse as it relies heavily on the

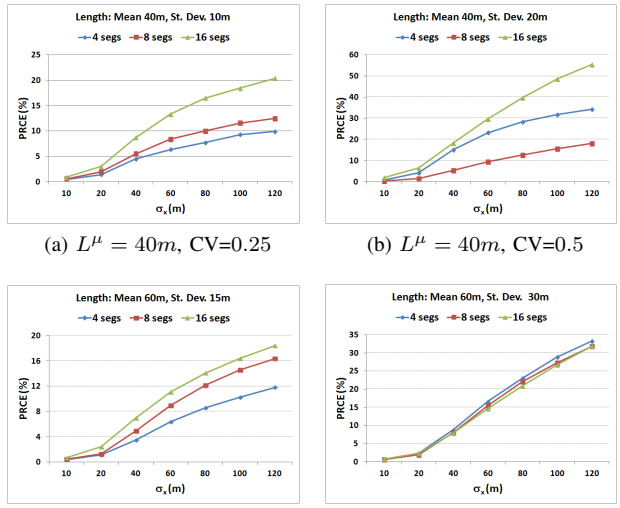

(a) $L^\mu = 40m$, CV=0.25 (b) $L^\mu = 40m$, CV=0.5

(c) $L^\mu = 60m$, CV=0.25 (d) $L^\mu = 60m$, CV=0.5

Fig. 4a. Relative gains on network of segments, under uniform noise.

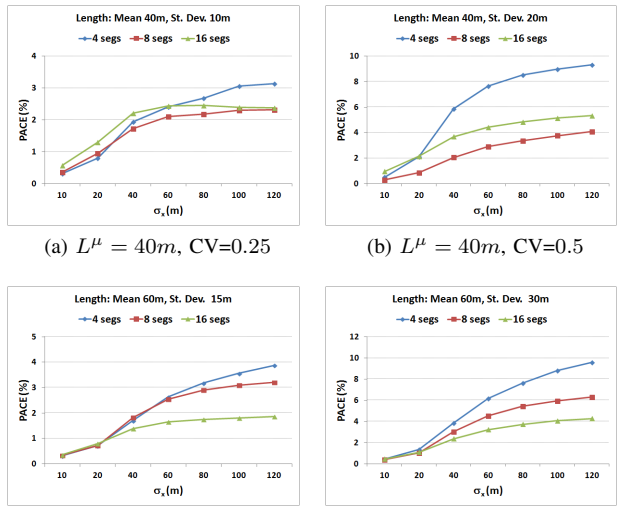

(a) $L^\mu = 40m$, CV=0.25 (b) $L^\mu = 40m$, CV=0.5

(c) $L^\mu = 60m$, CV=0.25 (d) $L^\mu = 60m$, CV=0.5

Fig. 4b. Absolute gains on network of segments, under uniform noise.

shortest distance, and, favors the nearest segment accordingly. The increasing gains are more pronounced depending on the variation in segment lengths, for instance, gains increasing quite quickly with increasing σ_x when CV is 1. Eventually, the gains seems to be stabilizing towards a limiting value.

Non-uniform noise distribution simulations compare measures (27) and (32), and the results are shown in Fig. 6a and 6b. The rows of subfigures again correspond to simulations with different average segments lengths, L^μ, and the curves with different colors again correspond to different number of segments. The columns correspond to different R values of $1, 0.7, 0.5$, and 0.2, and x-axis shows the standard deviation in x-direction, σ_x. All simulations were done for CV=1, since it was the case with the most gains under uniform noise simulations. In Fig. 6a, from left to right, slight drops in gains with decreasing R values can be observed; yet, the gains still remain quite high. Also, similar patterns about σ_x can be

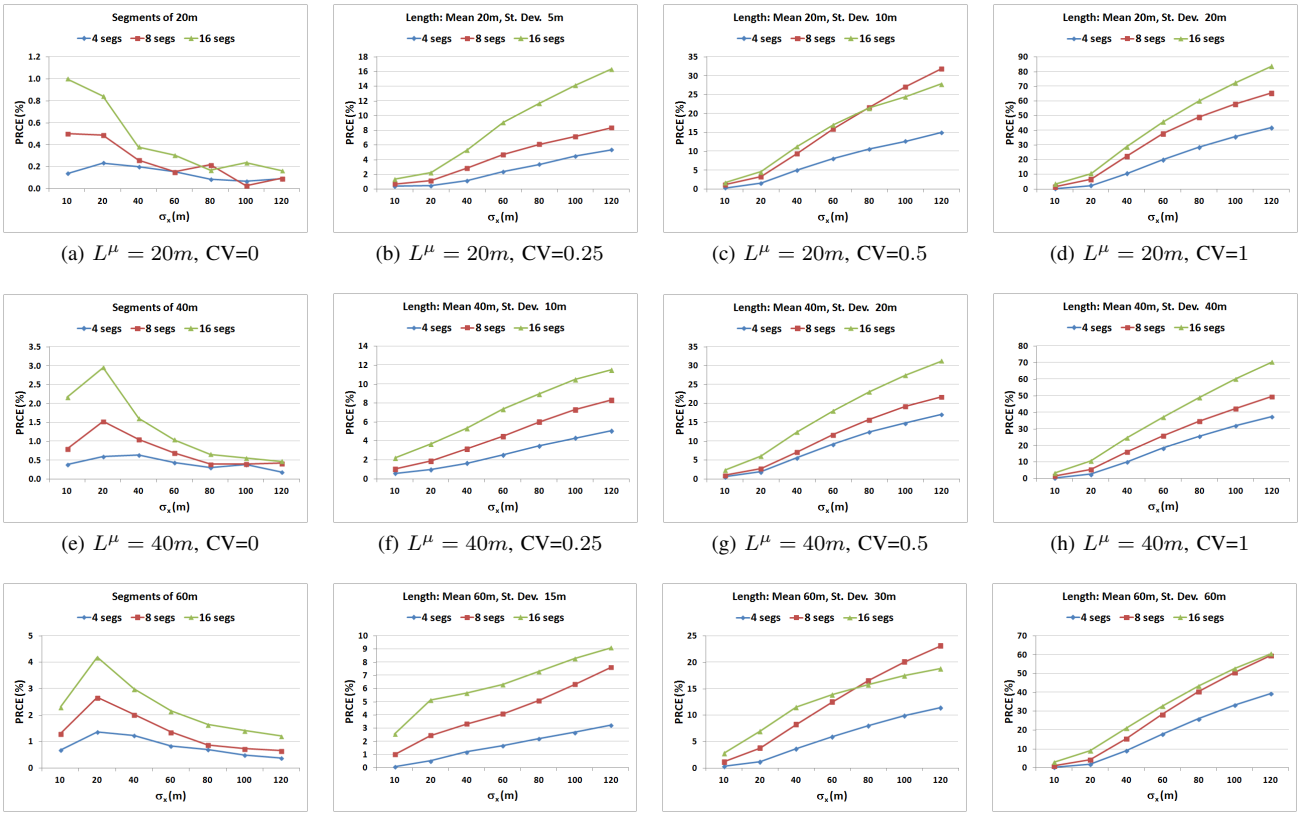

(a) $L^{\mu} = 20m$, CV=0 (b) $L^{\mu} = 20m$, CV=0.25 (c) $L^{\mu} = 20m$, CV=0.5 (d) $L^{\mu} = 20m$, CV=1

(e) $L^{\mu} = 40m$, CV=0 (f) $L^{\mu} = 40m$, CV=0.25 (g) $L^{\mu} = 40m$, CV=0.5 (h) $L^{\mu} = 40m$, CV=1

(i) $L^{\mu} = 60m$, CV=0 (j) $L^{\mu} = 60m$, CV=0.25 (k) $L^{\mu} = 60m$, CV=0.5 (l) $L^{\mu} = 60m$, CV=1

Fig. 5a. Relative gains on random segments, under uniform noise.

observed compared to Fig. 4a, and 5a. Hence, the proposed measures remain a better alternative under non-uniform noise distributions as well.

Also, in most tests, the gains are higher with more segments, as evidenced in Fig. 4a, 5a, and 6a (16 segments highest, followed by 8 and 4). Hence, the proposed measures will also be suitable for MM in urban centers with dense road networks.

Overall, the proposed proximity measures have yielded considerably better estimates, except the marginal gains for segments with equal lengths. The gains were higher with increasing variation in segment lenghts, noise standard deviation values, and the number of segments.

C. Computational Aspects

Switching to (27) from (32) or to (37) from (41) brings some extra computational time for the proximity analysis. The difference is that (27) and (37) are more complex functions, and will take more CPU time for computations. Yet, they also avoid the if-comparisons in (33), and (42). Therefore, the extra computations will not be very demanding. To have an idea about possible increase in computation efforts, we kept track of the computation times for some of our simulations. We have observed that the increase in computational time stayed between 8% to 20% of the original pointwise proximity computational times. Depending on the problem and the available data, this extra computational time can easily be justified for possible gains in estimation accuracy.

V. Conclusions

Building upon a careful analysis of the drawbacks of traditional pointwise proximity measures between a point and a curve, we have proposed the integral proximity measure that can reflect the likelihoods of the states of a stochastic process in a more consistent way. Assuming a generic stochastic model with additive noise, we have discussed the correct proximity function for proximity measures, and the relationship between a posteriori probabilities of the process and the proximity measures for a comparison of both measures. In addition, we have proved that the proposed integral proximity measure can yield better inferences than the pointwise measure for problems under the influence of uncorrelated bivariate Gaussian noise processes. Randomly generated Monte Carlo simulations also showed that absolute gains up to 18%, and relative gains up to 80% can be possible, with the additional computational times ranging between 8% to 20%.

Appendix A

Proof. With the noise process being zero-mean bivariate Gaussian, for a point $s(t)$ of segment S,

$$g_{\zeta}(p - s(t)) = \frac{1}{2\pi\sqrt{|\Sigma|}} e^{-\frac{1}{2}(p-s(t))^T \Sigma^{-1}(p-s(t))}. \quad (45)$$

Then, (14) becomes

$$W_I(p, S) = \frac{||L^S||}{2\pi\sqrt{|\Sigma|}} \int_0^1 e^{-\frac{1}{2}(p-s(t))^T \Sigma^{-1}(p-s(t))}\, dt. \quad (46)$$

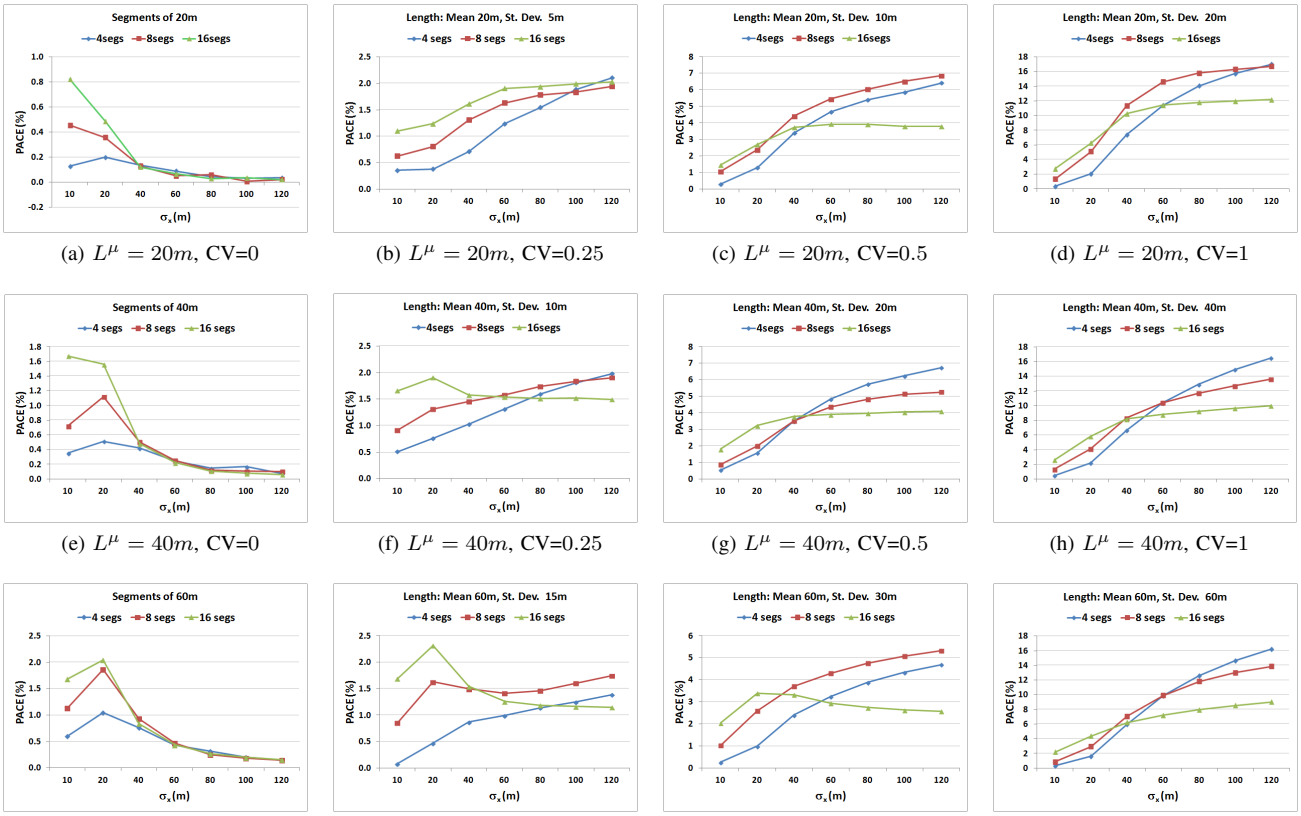

(a) $L^\mu = 20m$, CV=0 (b) $L^\mu = 20m$, CV=0.25 (c) $L^\mu = 20m$, CV=0.5 (d) $L^\mu = 20m$, CV=1

(e) $L^\mu = 40m$, CV=0 (f) $L^\mu = 40m$, CV=0.25 (g) $L^\mu = 40m$, CV=0.5 (h) $L^\mu = 40m$, CV=1

(i) $L^\mu = 60m$, CV=0 (j) $L^\mu = 60m$, CV=0.25 (k) $L^\mu = 60m$, CV=0.5 (l) $L^\mu = 60m$, CV=1

Fig. 5b. Absolute gains on random segments, under uniform noise.

Considering the parametrization of (10), and the inverse of the covariance matrix, the exponential term becomes,

$$[p - s(t)]^T \Sigma^{-1} [p - s(t)] = \tilde{A}t^2 + 2\tilde{B}t + \tilde{C}, \qquad (47)$$

where, $\tilde{A} \doteq ||\tilde{L}||^2, \quad \tilde{B} \doteq \tilde{R}^A \cdot \tilde{L}, \quad \tilde{C} \doteq ||\tilde{R}^A||^2,$ (48)

with $\tilde{R}^A$ and $\tilde{L}$ introduced in (25). Since,

$$\tilde{A}t^2 + 2\tilde{B}t + \tilde{C} = \tilde{A}(t + \tilde{B}/\tilde{A})^2 - \tilde{B}^2/\tilde{A} + \tilde{C},$$

(46) becomes,

$$W_I(p, S) = \frac{||L^S||}{2\,\pi\,\sigma_1\sigma_2} e^{(\tilde{B}^2/\tilde{A} - \tilde{C})/2} \int_0^1 e^{-\tilde{A}(t+\tilde{B}/\tilde{A})^2/2}\, dt. \qquad (49)$$

Doing change of variables with $x = \sqrt{\tilde{A}}\,(t + \tilde{B}/\tilde{A})$ yields:

$$\int_0^1 e^{-\tilde{A}(t+\tilde{B}/\tilde{A})^2/2}\, dt = \int_{\frac{\tilde{B}}{\sqrt{\tilde{A}}}}^{\frac{\tilde{A}+\tilde{B}}{\sqrt{\tilde{A}}}} e^{-x^2/2} \frac{1}{\sqrt{\tilde{A}}}\, dx$$
$$= \frac{\sqrt{2\pi}}{\sqrt{\tilde{A}}} \left[\Phi\left(\frac{\tilde{A}+\tilde{B}}{\sqrt{\tilde{A}}}\right) - \Phi\left(\frac{\tilde{B}}{\sqrt{\tilde{A}}}\right) \right].$$

$\sqrt{\tilde{A}}$ is $||\tilde{L}||$, and following (31)

$$\frac{\tilde{B}^2}{\tilde{A}} - \tilde{C} = \frac{(\tilde{R}^A \cdot \tilde{L})^2}{\tilde{L} \cdot \tilde{L}} - \tilde{R}^A \cdot \tilde{R}^A = ||\tilde{R}^A_{\tilde{L}\parallel}||^2 - ||\tilde{R}^A||^2.$$

Orthogonality of $\tilde{R}^A_{\tilde{L}\parallel}$ and $\tilde{R}^A_{\tilde{L}\perp}$ implies $\tilde{B}^2/\tilde{A} - \tilde{C}$ is $-||\tilde{R}^A_{\tilde{L}\perp}||^2$. Also, note that,

$$\tilde{A} + \tilde{B} = \tilde{L} \cdot \tilde{L} + \tilde{R}^A \cdot \tilde{L} = \tilde{L} \cdot (\tilde{L} + \tilde{R}^A) = \tilde{L} \cdot \tilde{R}^B.$$

Considering the unit vector $\tilde{l}$ of (26),

$$\Phi\left(\frac{\tilde{A}+\tilde{B}}{\sqrt{\tilde{A}}}\right) - \Phi\left(\frac{\tilde{B}}{\sqrt{\tilde{A}}}\right) = \Phi(\tilde{R}^B \cdot \tilde{l}) - \Phi(\tilde{R}^A \cdot \tilde{l}).$$

Using these identities in (49) yields (27). □

Appendix B

Proof. Having $F(p, s) = g_\zeta(p - s)$, and (6) with (45) yields,

$$W_P(p, S) = \max_{s(t)\in S} \left[\frac{1}{2\pi\,\sigma_1\sigma_2}\, e^{-\frac{1}{2}(p-s(t))^T \Sigma^{-1}(p-s(t))} \right].$$

The max is attained when $(p - s(t))^T \Sigma^{-1} (p - s(t))$ is minimized. Let us refer to this term as $d_\Sigma(p, s(t))$, and recall (47), where we had expanded it into a quadratic form. Considering that, $d_\Sigma(p, s(t))$ attains its minimum at $t^* \in [0, 1]$ such that,

$$t^* = \begin{cases} 0 & \text{if } -\tilde{B}/\tilde{A} \le 0 \\ -\tilde{B}/\tilde{A} & \text{if } 0 < -\tilde{B}/\tilde{A} < 1 \\ 1 & \text{if } -\tilde{B}/\tilde{A} \ge 1. \end{cases} \qquad (50)$$

Then, along with the identities in (48), one gets:

$$d_\Sigma(p, s(t^*)) = \begin{cases} \tilde{C} = ||\tilde{R}^A||^2, & \text{if } t^* = 0 \\ -\tilde{B}^2/\tilde{A} + \tilde{C} = ||\tilde{R}^A_{\tilde{L}\perp}||^2, & \text{if } t^* = -\tilde{B}/\tilde{A} \\ \tilde{A} + 2\tilde{B} + \tilde{C} = ||\tilde{R}^B||^2 & \text{if } t^* = 1, \end{cases}$$

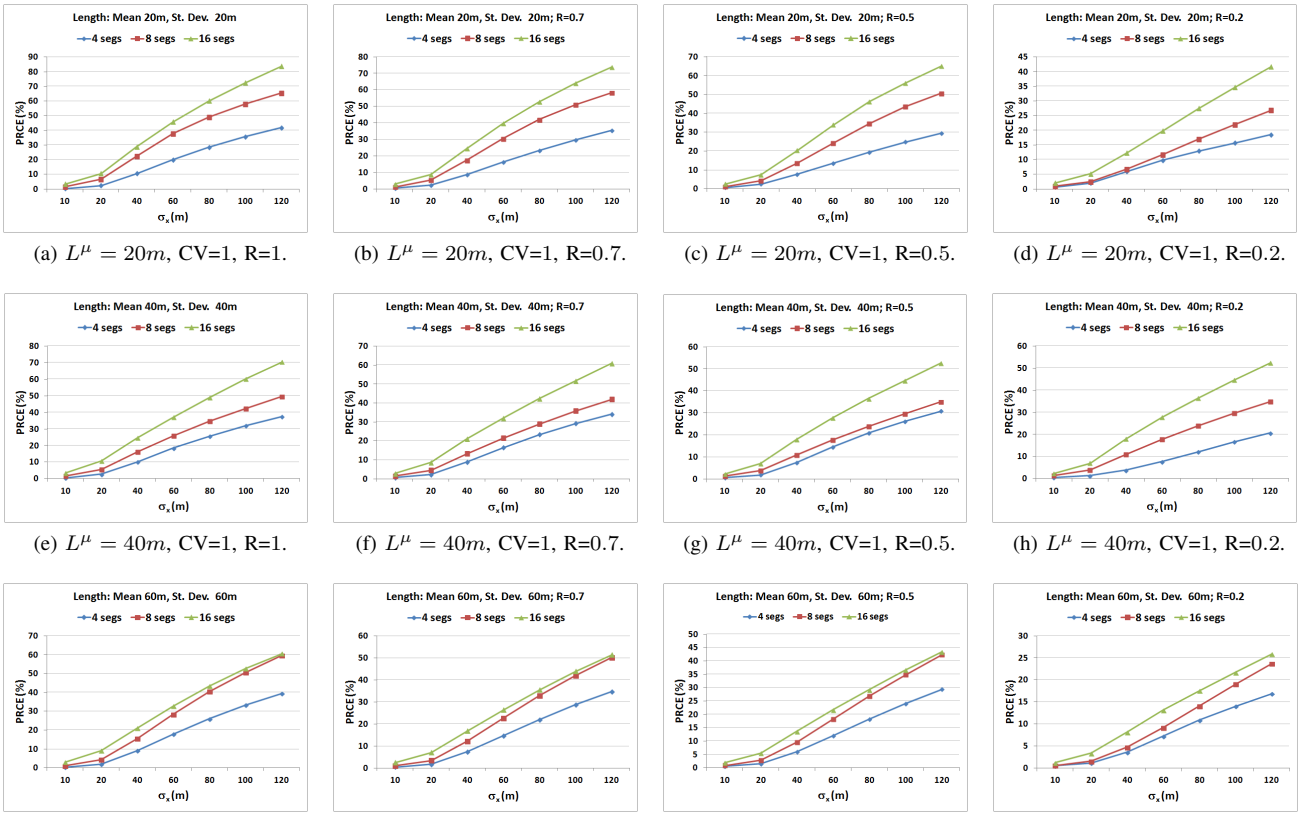

(a) $L^{\mu} = 20m$, CV=1, R=1. (b) $L^{\mu} = 20m$, CV=1, R=0.7. (c) $L^{\mu} = 20m$, CV=1, R=0.5. (d) $L^{\mu} = 20m$, CV=1, R=0.2.

(e) $L^{\mu} = 40m$, CV=1, R=1. (f) $L^{\mu} = 40m$, CV=1, R=0.7. (g) $L^{\mu} = 40m$, CV=1, R=0.5. (h) $L^{\mu} = 40m$, CV=1, R=0.2.

(i) $L^{\mu} = 60m$, CV=1, R=1. (j) $L^{\mu} = 60m$, CV=1, R=0.7. (k) $L^{\mu} = 60m$, CV=1, R=0.5. (l) $L^{\mu} = 60m$, CV=1, R=0.2.

Fig. 6a. Relative gains on random segments, under non-uniform noise.

and $\tilde{B}/\tilde{A} = \tilde{R} \cdot \tilde{l}/||\tilde{L}||$, which completes the proof. □

Appendix C

Proof. By choosing $F(p, s) = g_{\varsigma}(p - s)$, and following Lemma 1 and Lemma 2, under an uncorrelated non-degenerate bivariate Gaussian noise process, (34) will be defined by (32), and (35) by (27). Hence, we focus on equations (27), and (32).

For $W_I(p, S)$ in (27), let us first analyze its extrema points over all $p \in \mathbb{R}^2$. Note that $c(S)$ is independent p. Therefore, it is sufficient to analyze the product of $w^{\perp}(p, S)$ and $w^{\parallel}(p, S)$, which we will refer as $w(p, S)$.

$$\begin{aligned}\frac{d\,w(p,S)}{dp} &= \nabla w(p,S)\\ &= \nabla w^{\perp}(p,S)\, w^{\parallel}(p,S) + w^{\perp}(p,S)\, \nabla w^{\parallel}(p,S).\end{aligned}$$

Note that $w^{\perp}(p, S)$ and $w^{\parallel}(p, S)$ are orthogonal. Hence, the necessary condition, $\nabla w(p, S) = 0$, can only be satisfied when both $\nabla w^{\perp}(p, S)$ and $\nabla w^{\parallel}(p, S)$ are 0. Now,

$$\begin{aligned}\nabla w^{\perp}(p,S) &= \nabla e^{-||\tilde{R}^A_{\tilde{L}^{\perp}}||^2/2} = e^{-||\tilde{R}^A_{\tilde{L}^{\perp}}||^2/2} \nabla(-||\tilde{R}^A_{\tilde{L}^{\perp}}||^2/2),\\ \nabla(||\tilde{R}^A_{\tilde{L}^{\perp}}||^2) &= \nabla(\tilde{R}^A \cdot \tilde{l}_{\perp})^2 = 2(\tilde{R}^A \cdot \tilde{l}_{\perp})\nabla(\tilde{R}^A \cdot \tilde{l}_{\perp})\\ &= 2(\tilde{R}^A \cdot \tilde{l}_{\perp})(-\tilde{l}_{\perp}),\end{aligned}$$

where $\tilde{l}_{\perp}$ is the unit vector orthogonal to $\tilde{l}$. Then,

$$\nabla w^{\perp}(p,S) = e^{-||\tilde{R}^A_{\tilde{L}^{\perp}}||^2/2}(\tilde{R}^A \cdot \tilde{l}_{\perp})\tilde{l}_{\perp}.$$

Thus, the critical points of $w^{\perp}(p, S)$ satisfy $\tilde{R}^A \cdot \tilde{l}_{\perp} = 0$. Using the definitions of $\tilde{R}^A$ from (9) and (25), this holds for the set of points, $M^{\perp} \doteq \{p^* \in \mathbb{R}^2 : p^*(t) = S_A + t\,L, t \in (-\infty, \infty)\}$, where $w^{\perp}(p, S)$ attains its max. On the other hand,

$$\begin{aligned}\nabla w^{\parallel}(p,S) &= \nabla(\Phi(\tilde{R}^B \cdot \tilde{l}) - \Phi(\tilde{R}^A \cdot \tilde{l}))\\ &= \frac{1}{\sqrt{2\pi}} \nabla \left[\int_{\tilde{R}^A \cdot \tilde{l}}^{\tilde{R}^B \cdot \tilde{l}} e^{-x^2/2}\, dx \right]\end{aligned}$$

Using Leibniz rule,

$$\begin{aligned}\nabla w^{\parallel}(p,S) &= \frac{1}{\sqrt{2\pi}} \left[e^{-(\tilde{R}^B \cdot \tilde{l})^2} \nabla(\tilde{R}^B \cdot \tilde{l}) - e^{-(\tilde{R}^A \cdot \tilde{l})^2} \nabla(\tilde{R}^A \cdot \tilde{l}) \right]\\ &= \frac{1}{\sqrt{2\pi}} \left[e^{-(\tilde{R}^A \cdot \tilde{l})^2} - e^{-(\tilde{R}^B \cdot \tilde{l})^2} \right] \tilde{l}\end{aligned}$$

Thus, the critical points of $w^{\parallel}(p, S)$ satisfy $(\tilde{R}^A \cdot \tilde{l})^2 = (\tilde{R}^B \cdot \tilde{l})^2$. Then,

$$[(\tilde{R}^A \cdot \tilde{l}) - (\tilde{R}^B \cdot \tilde{l})][(\tilde{R}^A \cdot \tilde{l}) + (\tilde{R}^B \cdot \tilde{l})] = 0.$$

Using the definitions of $\tilde{R}^A$, $\tilde{R}^B$ from (9) and (25), one gets

$$[(\tilde{S}_A - \tilde{S}_B) \cdot \tilde{l}][(\tilde{S}_A + \tilde{S}_B - 2\tilde{p}) \cdot \tilde{l}] = 0.$$

This holds for the set of points, $M^{\parallel} \doteq \{p^* \in \mathbb{R}^2 : p^*(t) = (S_A + S_B)/2 + t\,L_{\perp}, t \in (-\infty, \infty)\}$, where $\nabla w^{\parallel}(p, S)$ attains its max. There is only one p^* that belongs to both $M^{\parallel}$ and $M^{\perp}$; and it is, $p^* = (S_A + S_B)/2$.

Thus, $w(p, S)$ has a unique global maximum, with no other extrema points. Hence, it is also strictly quasiconcave, and it

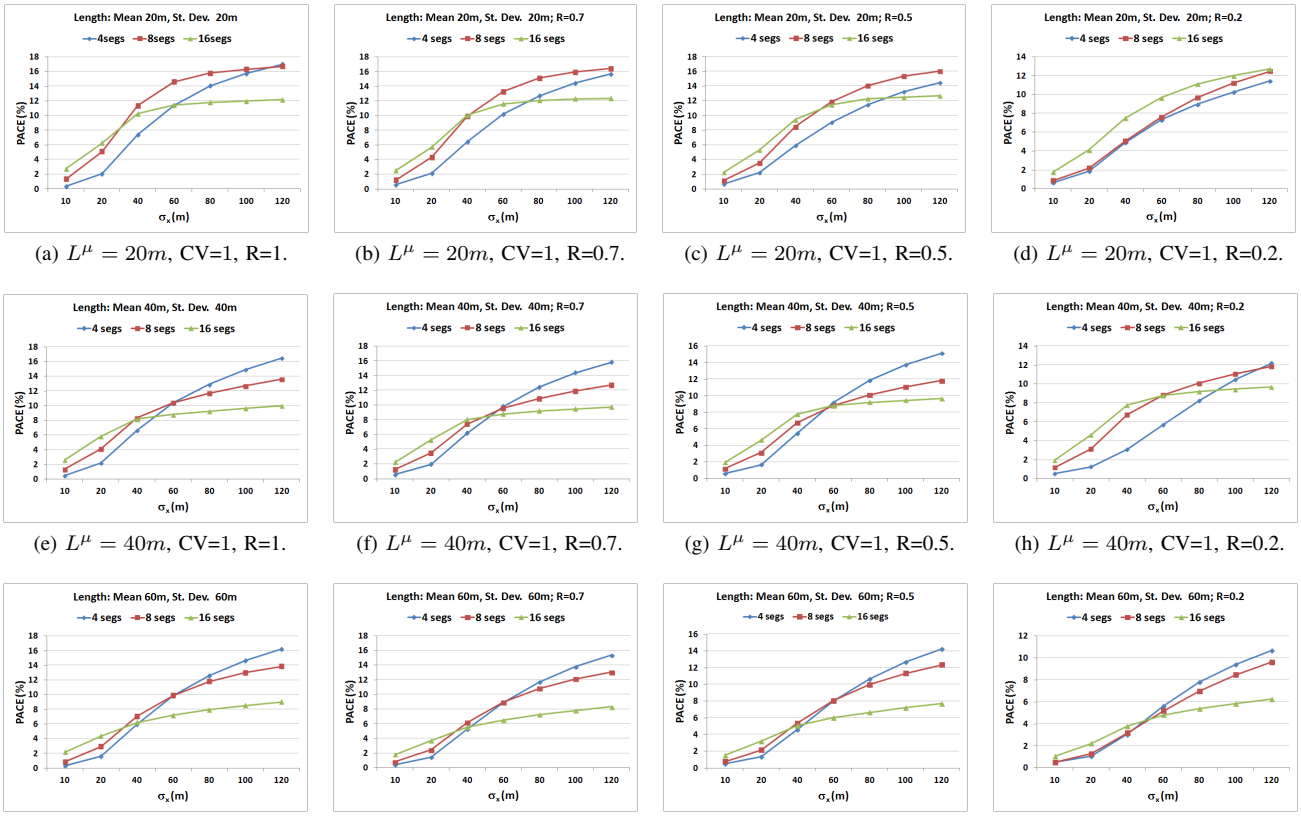

(a) $L^{\mu} = 20m$, CV=1, R=1. (b) $L^{\mu} = 20m$, CV=1, R=0.7. (c) $L^{\mu} = 20m$, CV=1, R=0.5. (d) $L^{\mu} = 20m$, CV=1, R=0.2.

(e) $L^{\mu} = 40m$, CV=1, R=1. (f) $L^{\mu} = 40m$, CV=1, R=0.7. (g) $L^{\mu} = 40m$, CV=1, R=0.5. (h) $L^{\mu} = 40m$, CV=1, R=0.2.

(i) $L^{\mu} = 60m$, CV=1, R=1. (j) $L^{\mu} = 60m$, CV=1, R=0.7. (k) $L^{\mu} = 60m$, CV=1, R=0.5. (l) $L^{\mu} = 60m$, CV=1, R=0.2.

Fig. 6b. Absolute gains on random segments, under non-uniform noise.

can not have thick level curves [52], [53]. Because of this, for two non-overlapping segments, S_1 and S_2, the set of points where $W_I(p, S_1)$ and $W_I(p, S_2)$ intersect, that is,

$$\{p \in \mathbb{R}^2 : \max_{s \in S_1} W_I(p, S_1) = \max_{s \in S_2} W_I(p, S_2)\}$$

can only define a curve but not a surface. Hence, (35) provides unique estimates for all points $p \in \mathbb{R}^2$ other than these points yielding equal value, thus allowing uniqueness almost surely.

In (32), $W_P(p, S)$ is defined by the piecewise exponential $v(p, S)$. For some segment S, the first two pieces of $v(p, S)$ attain their unique global maximum values at segment's end points, $p = S_A$ and $p = S_B$. The last piece of $v(p, S)$ is again $w^{\perp}(p, S)$, and we have just showed that it attains its global max for $p \in M^{\perp}$, the set of points along vector L. Therefore, (33) defines a semi-strictly-quasiconcave function with a flat-top over segment S. Consequently, $W_P(p, S)$ can not have thick level curves as well. Because of this, for two non-overlapping segments, S_1 and S_2, the set of points where $W_P(p, S_1)$ and $W_P(p, S_2)$ intersect, that is

$$\{p \in \mathbb{R}^2 : \max_{s \in S_1} W_P(p, S_1) = \max_{s \in S_2} W_P(p, S_2)\}$$

can only define a curve but not a surface. Hence, (34) provides unique estimates for all points $p \in \mathbb{R}^2$ other than these points yielding equal value, thus allowing uniqueness almost surely.

For the second half of the proof, let us introduce $\bar{R}^P$, and $\bar{R}^I$ to denote the set of points of non-unique results by (34) and (35), respectively. Also, let us define, sets of unique results for a segment $S_i \in \mathcal{S}$ as $\mathbb{R}_P(S_i) \doteq \{x : S_i = E^P(x, \mathcal{S})\}$, and $\mathbb{R}_I(S_i) \doteq \{x : S_i = E^I(x, \mathcal{S})\}$. Using the above sets, $\mathbb{R}^2$ can be partitioned by either of the following identities,

$$\bigcup_{S_i} \mathbb{R}_P(S_i) \cup \bar{\mathbb{R}}_P = \mathbb{R}^2, \quad \bigcup_{S_i} \mathbb{R}_I(S_i) \cup \bar{\mathbb{R}}_I = \mathbb{R}^2. \tag{51}$$

We also define the following disjoint sets for a segment, S_i,

$$\begin{aligned} Z^1(S_i) &\doteq \mathbb{R}_P(S_i) \cap \mathbb{R}_I(S_i), \\ Z^2(S_i) &\doteq \mathbb{R}_P(S_i) \setminus \left[\mathbb{R}_I(S_i) \cup \bar{\mathbb{R}}_I\right], \\ Z^3(S_i) &\doteq \mathbb{R}_I(S_i) \setminus \left[\mathbb{R}_P(S_i) \cup \bar{\mathbb{R}}_P\right]. \end{aligned} \tag{52}$$

$Z^1(S_i)$ is the set of points for which S_i is estimated as the original segment uniquely, by both estimators. $Z^2(S_i)$ is the set of points for which S_i is estimated as the original segment uniquely only by E^P, and $Z^3(S_i)$ only by E^I.

Lemma 3. *For $S_i \in \mathcal{S}$, $Z^3(S_i)$ can be partitioned as follows,*

$$Z^3(S_i) = \bigcup_{j \neq i} \left[Z^3(S_i) \cap Z^2(S_j)\right], \quad \bigcap_{j} Z^2(S_j) = \emptyset.$$

Proof. For $x \in Z^3(S_i)$, by (52), $x \notin \mathbb{R}_P(S_i)$, and $x \notin \bar{\mathbb{R}}_P$. By (51), $\exists\, k \neq i$ such that $x \in \mathbb{R}_P(S_k)$. Since $x \notin \mathbb{R}_I(S_k)$, $x \in Z^2(S_k)$, which implies $x \in Z^3(S_i) \cap (Z^2(S_k)$.

Since x was any point in $Z^3(S_i)$, $\forall x \in Z^3(S_i)$, $\exists\, S_j \in \mathcal{S}$, $j \neq i$, such that $x \in Z^2(S_j) \cap Z^3(S_i)$. $\square$

Lemma 4. *For $S_i \in \mathcal{S}$, $Z^2(S_i)$ can be partitioned as follows,*

$$Z^2(S_i) = \bigcup_{j \neq i} \left[Z^2(S_i) \cap Z^3(S_j) \right], \quad \bigcap_j Z^3(S_j) = \emptyset.$$

Proof. Follows the same argument in proof of Lemma 3. □

Following the definition of $\mathbb{R}_I(S_i)$ and $\mathbb{R}_P(S_i)$, the left and right terms of (36) can be expressed as:

$$Pr(E^I(p, \mathcal{S}) = S^p) = Pr(p \in \mathbb{R}_I(S^p)). \tag{53}$$

$$Pr(E^P(p, \mathcal{S}) = S^p) = Pr(p \in \mathbb{R}_P(S^p)). \tag{54}$$

Since the segments are non-overlapping, there can be only a finite number of intersection points between segments, and hence the probability of ξ being on those common points will be zero. Therefore, by excluding the intersection points $\mathcal{S}$ could be considered as a union of disjoint segments, and $\sum_i Pr(\xi \in S_i) = 1$. By the law of total probability,

$$Pr(p \in \mathbb{R}_I(S^p)) = \sum_i \left[Pr(p \in \mathbb{R}_I(S_i) | \, \xi \in S_i) \right] Pr(\xi \in S_i), \tag{55}$$

$$Pr(p \in \mathbb{R}_P(S^p)) = \sum_i \left[Pr(p \in \mathbb{R}_P(S_i) | \, \xi \in S_i) \right] Pr(\xi \in S_i). \tag{56}$$

To shorten the notation, let

$$p^i \doteq p = \xi + \zeta, \text{ such that}, \xi \in S_i. \tag{57}$$

From (52), $\mathbb{R}_I(S^p) = Z^1(S^p) \cup Z^3(S^p)$, and $\mathbb{R}_P(S^p) = Z^1(S^p) \cup Z^2(S^p)$. Therefore, along with (57),

$$Pr\left(p \in \mathbb{R}_I(S^p)\right) = \sum_i \left[Pr(p^i \in Z^1(S_i)) + Pr(p^i \in Z^3(S_i)) \right] Pr(\xi \in S_i), \tag{58}$$

$$Pr\left(p \in \mathbb{R}_P(S^p)\right) = \sum_i \left[Pr(p^i \in Z^1(S_i)) + Pr(p^i \in Z^2(S_i)) \right] Pr(\xi \in S_i). \tag{59}$$

Following (58) and (59), (36) is equivalent to,

$$\sum_i \left[Pr(p^i \in Z^1(S_i)) + Pr(p^i \in Z^3(S_i)) \right] Pr(\xi \in S_i) > \sum_i \left[Pr(p^i \in Z^1(S_i)) + Pr(p^i \in Z^2(S_i)) \right] Pr(\xi \in S_i).$$

After omitting common terms with $Z^1(S_i)$, we get,

$$\sum_i Pr\left(p^i \in Z^3(S_i)\right) Pr(\xi \in S_i) > \sum_i Pr\left(p^i \in Z^2(S_i)\right) Pr(\xi \in S_i). \tag{60}$$

ξ is uniformly distributed on the segments, and hence,

$$g_\xi(z) = \begin{cases} \frac{1}{\sum_{S_i} ||L^{S_i}||} & \text{if } z \in S, S \in \mathcal{S}, \\ 0 & \text{else.} \end{cases} \tag{61}$$

Let us introduce $k \doteq \sum_{S^i} ||L^{S_i}||$, and define $g_\xi(z) = 1/k$, for z on segments. This yields, $Pr(\xi \in S_i) = ||L^{S_i}||/k$.

From (57), $g_{p^i}(z) = g_{\xi+\zeta}(z | \, \xi \in S_i)$; and ζ is independent of ξ. Since pdf of the sum of two independent random variables can be formulated by the convolution of their pdfs, $g_{p^i}(z) = g_\xi(z | \xi \in S_i) * g_\zeta(z)$, with the convolution integral defined on S_i. That is,

$$g_{p^i}(z) = g_\xi(z | \, \xi \in S_i) * g_\zeta(z) = \int_{S_i} g_\zeta(z-u) \, g_\xi(u | \, \xi \in S_i) \, du = \int_{S_i} g_\zeta(z-u) \, \frac{1}{||L^{S_i}||} \, du.$$

Accordingly, $Pr(p^i \in Z^3(S_i)$ in (60) can be written as,

$$Pr\left(p^i \in Z^3(S_i)\right) = \int_{Z^3(S_i)} \int_{S_i} g_\zeta(z-u) \, \frac{1}{||L^{S_i}||} \, du \, dz.$$

By formulating $Pr(p^i \in Z^2(S_i)$ in a similar fashion, and using (61) for $Pr(\xi \in S_i)$, (60) becomes,

$$\sum_i \int_{Z^3(S_i)} \left[\int_{S_i} g_\zeta(z-u) \, \frac{1}{||L^{S_i}||} \, du \right] dz \, \frac{||L^{S_i}||}{k} > \sum_i \int_{Z^2(S_i)} \left[\int_{S_i} g_\zeta(z-u) \, \frac{1}{||L^{S_i}||} \, du \right] dz \, \frac{||L^{S_i}||}{k}.$$

Omitting the common terms with $1/k$, and reordering, the needed condition becomes,

$$\sum_i \left[\int_{Z^3(S_i)} \int_{S_i} g_\zeta(z-u) \, du \, dz - \int_{Z^2(S_i)} \int_{S_i} g_\zeta(z-u) \, du \, dz \right] > 0. \tag{62}$$

From Lemma 3, Lemma 4, we know that $\forall S_i \in \mathcal{S}$, $\forall z \in Z^3(S_i), \exists \, Z^2(S_j), j \neq i$, such that $z \in Z^2(S_i)$; and similarly $\forall z \in Z^2(S_i), \exists \, Z^3(S_j), j \neq i$, such that $z \in Z^3(S_i)$. Therefore, we can expand $Z^3(S_i)$ and $Z^2(S_i)$; and regroup the integrals to get,

$$\sum_i \sum_j \int_{Z^3(S_i) \cap Z^2(S_j)} \left[\int_{S_i} g_\zeta(z-u) \, du - \int_{S_j} g_\zeta(z-u) \, du \right] dz > 0. \tag{63}$$

Yet, from the definition of $Z^3(S_i)$ and $Z^2(S_j)$, $\forall (S_i, S_j) \in \mathcal{S} \times \mathcal{S}$, $\forall z \in Z^3(S_i) \cap Z^2(S_j)$, the following is already satisfied,

$$\int_{S_i} g_\zeta(z-u) \, du - \int_{S_j} g_\zeta(z-u) \, du > 0.$$

Hence, the necessary inequality holds. □

References

[1] M. A. Quddus, W. Y. Ochieng, and R. B. Noland, "Current map-matching algorithms for transport applications: State-of-the art and future research directions," *Transportation Research Part C: Emerging Technologies*, vol. 15, no. 5, pp. 312 – 328, 2007.

[2] M. Hashemi and H. A. Karimi, "A critical review of real-time map-matching algorithms: Current issues and future directions," *Computers, Environment and Urban Systems*, vol. 48, pp. 153 – 165, 2014.

[3] J. S. Greenfeld, "Matching gps observations to locations on a digital map," in *Transportation Research Board 81st Annual Meeting*, 2002.

[4] C. E. White, D. Bernstein, and A. L. Kornhauser, "Some map matching algorithms for personal navigation assistants," *Transportation Research Part C: Emerging Technologies*, vol. 8, no. 16, pp. 91 – 108, 2000.

[5] L. Zhao, W. Y. Ochieng, M. A. Quddus, and R. B. Noland, "An extended Kalman filter algorithm for integrating gps and low cost dead reckoning system data for vehicle performance and emissions monitoring," *The J. of Navigation*, vol. 56, pp. 257–275, 5 2003.

[6] F. Marchal, J. Hackney, and K. Axhausen, "Efficient map matching of large global positioning system data sets: Tests on speed-monitoring experiment in Zürich," *Transportation Research Record: J. of the Transportation Research Board*, vol. 1935, pp. 93–100, 2005.

[7] D. Obradovic, H. Lenz, and M. Schupfner, "Fusion of sensor data in Siemens car navigation system," *IEEE Trans. on Vehicular Technology*, vol. 56, no. 1, pp. 43–50, 2007.

[8] M. A. Quddus, R. B. Noland, and W. Y. Ochieng, "A high accuracy fuzzy logic based map matching algorithm for road transport," *J. of Intelligent Transportation Syst.*, vol. 10, no. 3, pp. 103–115, 2006.

[9] G. Jagadeesh, T. Srikanthan, and X. Zhang, "A map matching method for gps based real-time vehicle location," *J. of Navigation*, vol. 57, no. 03, pp. 429–440, 2004.

[10] W. Ochieng, M. Quddus, and R. Noland, "Map-matching in complex urban road networks," *Brazilian Journal of Cartography (Revista Brasileira de Cartografia)*, vol. 55, no. 2, pp. 1–18, 2003.

[11] N. Tradisauskas, J. Juhl, H. Lahrmann, and C. Jensen, "Map matching for intelligent speed adaptation," *IET Intelligent Transport Syst.*, vol. 3, no. 1, pp. 57–66, 2009.

[12] N. R. Velaga, M. A. Quddus, and A. L. Bristow, "Developing an enhanced weight-based topological map-matching algorithm for intelligent transport systems," *Transportation Research Part C: Emerging Technologies*, vol. 17, no. 6, pp. 672 – 683, 2009.

[13] C. Smaili, M. E. El Najjar, and F. Charpillet, "A road matching method for precise vehicle localization using hybrid Bayesian network," *J. of Intelligent Transportation Syst.*, vol. 12, no. 4, pp. 176–188, 2008.

[14] R. Toledo-Moreo, D. Betaille, and F. Peyret, "Lane-level integrity provision for navigation and map matching with GNSS, dead reckoning, and enhanced maps," *IEEE Trans. on Intell. Transp. Syst.*, vol. 11, no. 1, pp. 100–112, 2010.

[15] M. M. Atia, A. R. Hilal, C. Stellings, E. Hartwell, J. Toonstra, W. B. Miners, and O. A. Basir, "A low-cost lane-determination system using GNSS/IMU fusion and hmm-based multistage map matching," *IEEE Trans. on Intell. Transp. Syst.*, vol. PP, no. 99, pp. 1–11, 2017.

[16] J. Biagioni, T. Gerlich, T. Merrifield, and J. Eriksson, "Easytracker: Automatic transit tracking, mapping, and arrival time prediction using smartphones," in *Proc. of ACM Conf. on Embedded Networked Sensor Syst.*, 2011, pp. 68–81.

[17] J. Han, E. Owusu, L. Nguyen, A. Perrig, and J. Zhang, "Accomplice: Location inference using accelerometers on smartphones," in *Proc. of Int. Conf. on Communication Systems and Networks*, 2012, pp. 1–9.

[18] M. Lv, L. Chen, X. Wu, and G. Chen, "A road congestion detection system using undedicated mobile phones," *IEEE Trans. on Intell. Transp. Syst.*, vol. 16, no. 6, pp. 3060–3072, 2015.

[19] M. Bierlaire, J. Chen, and J. Newman, "A probabilistic map matching method for smartphone GPS data," *Transportation Research Part C: Emerging Technologies*, vol. 26, no. 0, pp. 78 – 98, 2013.

[20] T. Hunter, P. Abbeel, and A. Bayen, "The path inference filter: Model-based low-latency map matching of probe vehicle data," *IEEE Trans. on Intell. Transp. Syst.*, vol. 15, no. 2, pp. 507–529, 2014.

[21] G. R. Jagadeesh and T. Srikanthan, "Online map-matching of noisy and sparse location data with hidden markov and route choice models," *IEEE Trans. on Intell. Transp. Syst.*, no. 99, pp. 1–12, 2017.

[22] S. Brakatsoulas, D. Pfoser, R. Salas, and C. Wenk, "On map-matching vehicle tracking data," in *Proc. of Int. Conf. on Very large data*. VLDB Endowment, 2005, pp. 853–864.

[23] D. Pfoser and C. S. Jensen, "Capturing the uncertainty of moving-object representations," in *Proc. of Int. Symp. on Advances in Spatial Databases*, 1999, pp. 111–132.

[24] F. Gustafsson, F. Gunnarsson, N. Bergman, U. Forssell, J. Jansson, R. Karlsson, and P.-J. Nordlund, "Particle filters for positioning, navigation, and tracking," *IEEE Trans. on Signal Processing*, vol. 50, no. 2, pp. 425–437, 2002.

[25] I. Skog and P. Handel, "In-car positioning and navigation technologies– a survey," *IEEE Trans. on Intell. Transp. Syst.*, vol. 10, no. 1, pp. 4–21, March 2009.

[26] M. Quddus, W. Ochieng, L. Zhao, and R. Noland, "A general map matching algorithm for transport telematics applications," *GPS Solutions*, vol. 7, pp. 157–167, 2003.

[27] J.-s. Yang, S.-p. Kang, and K.-s. Chon, "The map matching algorithm of GPS data with relatively long polling time intervals," *J. of the Eastern Asia Society for Transportation Studies*, vol. 6, pp. 2561–2573, 2005.

[28] F. Diggelen, "System design & test-GNSS accuracy-lies, damn lies, and statistics," *GPS World*, vol. 18, no. 1, pp. 26–33, 2007.

[29] P. Newson and J. Krumm, "Hidden markov map matching through noise and sparseness," in *Proc. of ACM SIGSPATIAL Int. Conf. on Advances in Geographic Information Syst.*, 2009, pp. 336–343.

[30] Y. Lou, C. Zhang, Y. Zheng, X. Xie, W. Wang, and Y. Huang, "Map-matching for low-sampling-rate GPS trajectories," in *Proc. of ACM SIGSPATIAL Int. Conf. on Adv. in Geo. Inform. Syst.*, 2009, pp. 352–361.

[31] C. Goh, J. Dauwels, N. Mitrovic, M. T. Asif, A. Oran, and P. Jaillet, "Online map-matching based on Hidden Markov model for real-time traffic sensing applications," in *Proc. of Int. IEEE Conf. on Intelligent Transportation Syst.*, 2012, pp. 776 –781.

[32] J. Yuan, Y. Zheng, C. Zhang, X. Xie, and G.-Z. Sun, "An interactive-voting based map matching algorithm," in *Proc. of Int. Conf. on Mobile Data Management*. IEEE Computer Society, 2010, pp. 43–52.

[33] X. Liu, K. Liu, M. Li, and F. Lu, "A st-crf map-matching method for low-frequency floating car data," *IEEE Trans. on Intell. Transp. Syst.*, vol. 18, no. 5, pp. 1241–1254, 2017.

[34] O. Mazhelis, "Using recursive Bayesian estimation for matching GPS measurements to imperfect road network data," in *Proc. of Int. IEEE Conf. on Intelligent Transportation Syst.*, 2010, pp. 1492–1497.

[35] G. Jagadeesh and T. Srikanthan, "Robust real-time route inference from sparse vehicle position data," in *Proc. of IEEE Int. Conf. on Intelligent Transportation Syst.*, Oct 2014, pp. 296–301.

[36] M. Quddus and S. Washington, "Shortest path and vehicle trajectory aided map-matching for low frequency {GPS} data," *Transportation Research Part C: Emerging Technologies*, vol. 55, pp. 328 – 339, 2015.

[37] R. Mohamed, H. Aly, and M. Youssef, "Accurate real-time map matching for challenging environments," *IEEE Trans. on Intell. Transp. Syst.*, vol. 18, no. 4, pp. 847–857, 2017.

[38] M. Hashemi and H. A. Karimi, "A weight-based map-matching algorithm for vehicle navigation in complex urban networks," *Journal of Intell. Transp. Syst.*, vol. 20, no. 6, pp. 573–590, 2016.

[39] G. Hu, J. Shao, F. Liu, Y. Wang, and H. T. Shen, "If-matching: Towards accurate map-matching with information fusion," *IEEE Trans. on Knowledge and Data Engineering*, vol. 29, no. 1, pp. 114–127, 2017.

[40] Y. J. Gong, E. Chen, X. Zhang, L. M. Ni, and J. Zhang, "Antmapper: An ant colony-based map matching approach for trajectory-based applications," *IEEE Trans. on Intell. Transp. Syst.*, no. 99, pp. 1–12, 2017.

[41] H. Wei, Y. Wang, G. Forman, and Y. Zhu, "Map matching by Fréchet distance and global weight optimization," *Technical Paper, Departement of Computer Science and Engineering*, 2013.

[42] O. Pink and B. Hummel, "A statistical approach to map matching using road network geometry, topology and vehicular motion constraints," in *Proc. of Int. IEEE Conf. on Intell. Transp. Syst.*, 2008, pp. 862–867.

[43] A. Oran and P. Jaillet, "A precise proximity-weight formulation for map matching algorithms," in *Proc. of Workshop on Positioning Navigation and Communication*, 2013, pp. 1–6.

[44] R. Assam and T. Seidl, "Private map matching: Realistic private route cognition on road networks," in *Proc. of IEEE Int. Conf. on Ubiquitous Intelligence and Computing, and Int. Conf. on Autonomic and Trusted Computing*, 2013, pp. 178–185.

[45] A. Oran and P. Jaillet, "An HMM-based map matching method with cumulative proximity-weight formulation," in *Proc. of Int. Conf. on Connected Vehicles and Expo*, 2013, pp. 480–485.

[46] M. Bierlaire and E. Frejinger, "Route choice modeling with network-free data," *Transportation Research Part C: Emerging Technologies*, vol. 16, no. 2, pp. 187 – 198, 2008.

[47] P. Y. Simard, Y. A. Le Cun, J. S. Denker, and B. Victorri, "Transformation invariance in pattern recognition: Tangent distance and propagation," *Int. J. of Imaging Syst. and Technol.*, vol. 11, no. 3, pp. 181–197, 2000.

[48] J. W. Dettman, *Applied Complex Variables*. Dover, 1984, ch. 1.6.

[49] A. N. Michel and C. J. Herget, *Applied Algebra and Functional Analysis*. Dover, 1993, ch. 5.

[50] R. Mahler, ""Statistics 101" for multisensor, multitarget data fusion," *IEEE Aerosp. and Electron. Syst. Mag.*, vol. 19, no. 1, pp. 53–64, 2004.

[51] A. A. Hagberg, D. A. Schult, and P. J. Swart, "Exploring network structure, dynamics, and function using NetworkX," in *Proc. of the 7th Python in Science Conf.*, 2008, pp. 11–15.

[52] M. Avriel, W. Diewert, S. Schaible, and I. Zang, *Generalized Concavity*. Society for Industrial and Applied Mathematics, 2010, ch. 3.

[53] W. Diewert, M. Avriel, and I. Zang, "Nine kinds of quasiconcavity and concavity," *J. of Economic Theory*, vol. 25, no. 3, pp. 397 – 420, 1981.

Ali Oran received his masters and doctoral degrees from University of California, San Diego in 2005, and 2010, respectively. Following his graduation, he joined the Future Urban Mobility Group at Singapore Massachusetts Institute of Technology Alliance for Research Technology (SMART) Center. Currently, he is with the University of Colorado, Boulder. His research interests include vehicle localization, vehicle routing, decision making under uncertainty, and statistical inference.

Patrick Jaillet received the Ph.D. degree in operations research from the Massachusetts Institute of Technology, Cambridge, MA, USA, in 1985. He is currently the Dugald C. Jackson Professor of the Department of Electrical Engineering and Computer Science, School of Engineering, and a Codirector of the Operations Research Center, Massachusetts Institute of Technology. His research interests include algorithm design and analysis for online problems, real-time and dynamic optimization, network design and optimization, and probabilistic combinatorial optimization.